



Preparation and performance in IR and UV of transparent inorganic polysiloxane coating with dispersed TiO_2 on glass substrates

S.A. Saudi, A.F. Mohd *

School of Industrial Technology, Department of Polymer Chemistry Science and Technology, Faculty of Applied Sciences, University of Technology MARA (UiTM), 40450, Shah Alam, Malaysia

* Corresponding e-mail address: ahmadfaiza@uitm.edu.my

ORCID identifier:  <https://orcid.org/0000-0001-8625-1457> (S.A.S.)

ABSTRACT

Purpose: The aim of the presented work was to develop an economical, transparent coating with dispersed TiO_2 dispersion and inorganic polysiloxane resin for glass windows application and to study its effectiveness in filtering IR and UV radiations.

Design/methodology/approach: Two oligomeric silanes were prepared in different molar ratios to produce inorganic polysiloxane resin. They were tested for their viscosity to reflect the completion of the reaction and form an amide linkage. FTIR was done to support the viscosity result by proving the presence of amide linkages. 10%, 20%, and 30% of compounded TiO_2 were successfully dispersed in 0.3% sodium sulfosalicylate (dehydrated ethanol). Each TiO_2 concentration was characterized for size distribution and polydispersity index (PDI). Additives solutions of 2-hydroxybenzophenone (HBP) and boron trifluoride (BF_3) were also soluted in the same solvent. Glass substrates were coated with the formulations and tested for curing and hardness properties. Windows Energy Profiler (WEP) was used to study the UV, IR, and daylight transmission of the coated glasses.

Findings: Each inorganic polysiloxane resin showed various viscosity values before reaching a constant state which designates complete formations of amide linkages. Polysiloxane resin with a viscosity value of 30.5 mPa/s was the most ideal to act as a binder. FTIR characterization proved the formation of amide linkages. The particle size distribution of TiO_2 recorded the size of 87 nm after dispersion with correlating value of 1 PDI. The fastest drying time of 3 hours was recorded. The pencil hardness test quoted 6H pencil as the hardest pencil grade. WEP analysis of UV, IR, and daylight transmission gives satisfactory results of 0%, 7%, and 61%, respectively.

Research limitations/implications: Laboratory analysis for viscosity tests often being held off. The test requires the samples to be transferred in a cylinder with an open-air spindle rotation. Samples react with the surrounding environment. Thus, polymerization takes place rapidly, resulting in hardened samples inside the cylinder. The different measure was taken by wrapping the testing area with aluminium foil. This research was conducted under equatorial climate.

Practical implications: The obtained test results may contribute to the conclusion of transparent TiO_2 nano-particles coating on glass substrates for windows application. This can reduce the electricity usage in buildings for artificial cooling to provide indoor thermal comfort. Smart coating formulations have a noticeable effect on filtering harmful solar radiation.



Originality/value: This study presents the economical and undemanding ways to develop transparent smart coating formulation with superior performance against solar radiation. It is expected to have a bright potential in the architectural industry.

Keywords: Transparent coating on glass substrates, TiO₂ dispersion, IR and UV shielding, Ultra-high shearing dispersion

Reference to this paper should be given in the following way:

S.A. Saudi, A.F. Mohd, Preparation and performance in IR and UV of transparent inorganic polysiloxane coating with dispersed TiO₂ on glass substrates, Journal of Achievements in Materials and Manufacturing Engineering 114/2 (2022) 49-56.

DOI: <https://doi.org/10.5604/01.3001.0016.2155>

PROPERTIES

1. Introduction

The transparent glass-based coating is a protective layer that exhibits low tint on glass substrates. The mighty sun radiates long-wavelength UV-A (315-400 nm) and short-wavelength UV-B (280-315 nm) to the earth's surface. Standard glass has an emittance of 0.84, indicating that only 17% of solar light is scattered, and the rest, 83%, is trapped [1]. Standard glass collects and transmits a lot of solar radiation and heat energy from the environment, creating thermal discomfort [1]. Glass windows must be coated to fabricate the problem of indoor heat accumulation due to harmful solar rays being radiated into buildings. It can be done by creating radiant barriers on glass windows to redirect the incoming rays. UV radiation induces photo-oxidative degradation, resulting in the production of radicals, the breaking of polymer chains and their molecular weight, as well as the loss of mechanical properties after an undetermined period [2]. Indoor furniture exposed to UV radiation will start to degrade as its chain network starts to break down. The effects of UV rays also contribute to DNA photo-damage [3]. UV rays trigger oxidative reactions, which spawn free radicals to stimulate reactive oxygen species (ROS) and discharge secondary radicals respective to their penetration depth [4]. Unfiltered UV-A can penetrate a human's dermis hence suppressing the immune system, whereas unfiltered UV-B may reach the superficial layer of human skin, thus inducing the development of skin cancer.

In this study, TiO₂ filters a significant amount of solar rays. Owing to its IR and UV absorption capability, TiO₂ improves the coating's weather resilience and absorbs UV rays, thus protecting the underlying resin molecules from UV damage [5]. TiO₂ in the coating allows for the unification of optical clarity and heat absorption characteristics, resulting in enhanced protection of coated surfaces [6]. Further improvement was made by incorporating a UV absorber of 2-hydroxybenzophenone (HBP) and boron trifluoride (BF₃) catalyst promoter into the

formulation. With HBP, coating degradation can be prevented, which often caused by harmful UV. The incident rays can also be absorbed to re-emits as low energy state.

Polysiloxane resin polymerized from two oligomeric silanes was used in this study to bind dissimilar materials of glass substrates and coating formulations. Polysiloxane is made with silicon monoxide (Si-O) in the backbone chain, which could considerably enhance and exhibit a high thermal efficiency [7].

The crosslinked network between the two silanes may impede any potential chain movement, and when heat is applied, the main network structure is prevented from deforming [8]. Aside from UV protection, inorganic coatings have great transmittance, resistant to water, oxygen, chemicals, and corrosion at high temperatures [9]. By coating glass substrates on buildings, advantages include energy savings, environmental and economical can be achieved [10].

2. Methodology

2.1. Preparation of inorganic polysiloxane resin

Polysiloxane resin was prepared from two dissimilar oligomeric silanes; epoxy-functional silane of (3-glycidyl-oxypropyl)trimethoxysilane and amino-functional silane hardener of (3-aminopropyl)triethoxysilane. Silanes were mixed and stirred at 1000 rpm for 5 hours following the ratios of 2:1, 1:2, and 1.5:2 with respect to the functional epoxy silane and amino-functional silane. This method was based on literature where epoxy-functional silanes of (3-metha-cryloxypropylmethyl-dimethoxysilane) and methyl-triethoxysilane are subsequently mixed with amino-functional silane of the same type to form ambient curable coating [11]. Samples were subjected to viscosity analysis using Brookfield Viscometer, model: DV-1 Prime Digital Viscometer by Ametek Brookfield in accordance with

ASTM D2857. The instrument was set to stir at 100 rpm at room temperature, and Spindle S-21 was used for all samples. The viscosity results were supported by FTIR spectroscopy characterization from Perkin Elmer.

2.2. Dispersion of functional additives

The dispersion method is tailored from a literature [12]. Compounded TiO₂ (300 nm) from United Kingdom and sodium sulfosalicylate dehydrated ethanol (240.17 g/mol, PubChem) were used as received

TiO₂ with 10%, 20% and 30% (w/v) were weighed and dispersed in 0.3% dehydrated ethanol. Additional grinding media of silica beads were added to the solvent. Ultra-shear high-speed disperser capable of re-circulating nano-particles was used. Dispersion medium was stirred for 5 minutes at 2000 rpm to create a large and stable vortex for particle shearing. TiO₂ was subsequently added to the solvent. Disperser speed was gradually increased to 5000 rpm following ASTM D6619 standard for high-speed dispersion.

After stirring, TiO₂ dispersions were left to stand to observe their stability. Samples were subjected to size distribution and polydispersity index (PDI) characterization using Particle Size Analyzer, model: Mastersizer 2000 by Azo Materials. The dispersion process and analyses were conducted at room temperature settings for all samples. Figure 1 shows the detailed flowchart.

The additives solution of powdered HBP was dispersed at 1000 rpm with BF₃ in the same solvent used to disperse TiO₂ additives. The solutions will be merged with TiO₂ concentrations to aid in the performance factor.

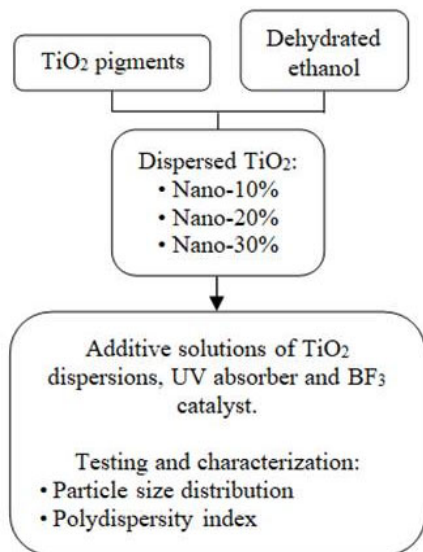


Fig. 1. Flowchart of TiO₂ dispersions and its testing

2.3. Curing analysis of inorganic polysiloxane resins

The prepared inorganic polysiloxane resin of different ratios integrated with the additives solutions was subjected to curing analysis. The test was conducted at room temperature with 50% humidity, following the ASTM D-1640 standard.

Ideal polysiloxane resin will be chosen from the curing test before merging it with the different TiO₂ concentrations, thus creating transparent coating formulations. Each formulation will be coated on glass substrates and subjected to a hardness test and energy transmission analysis.

2.4. Hardness and energy transmission properties

Coatings need to be tested for their hardness as part of the quality standards. Literature [13] and [14] used the surface micro-hardness method.

It is suitable to evaluate solid samples and coatings up to 1 m in length, with a force of 0.1 mN – 2 N. In this study, the pencil hardness method was preferred to determine the samples quality.

Pencils with different hardness grades manufactured by Faber Castell were used to scratch the coated film on the glass. The test starts from the hardest to softest pencil grade, following the ASTM D3363 standard. Pencils were pushed against the coated surface at a 45° angle under constant force. Sample was deemed as a 'fail' if the surface produced a scratch of 3 mm (Fig. 2).



Fig. 2. Scratched or failed sample in the pencil hardness test

To further understand the performance of coating formulations on IR and UV filtration, Windows Energy Profiler (WEP) instrument, model: WP4500, by EDTM was used. WEP can assess three types of real-time measurement; UV rays Transmission, near IR Transmission and Visible Light Transmission (VT). The flowchart in Figure 3 shows the related testing for the coating formulations.

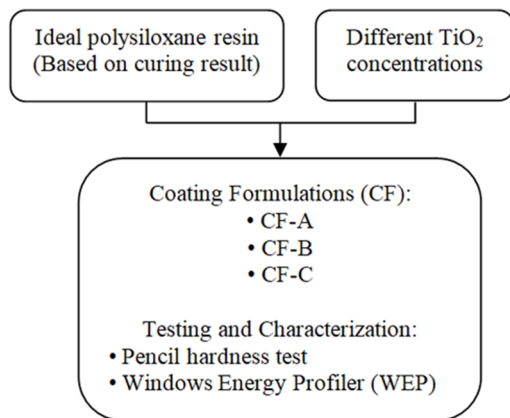


Fig. 3. Flowchart of coating formulations and their testing

3. Results and discussions

3.1. Viscosity test of inorganic polysiloxane resin

A series of polysiloxane resins were prepared between epoxy-functional silane and amino-functional silane hardeners. The polymerization occurs between hydroxyl and amine groups of respected silanes to allow chain opening by active hydrogen where oligomers will be attached to end-to-end, thus creating robust crosslink [15].

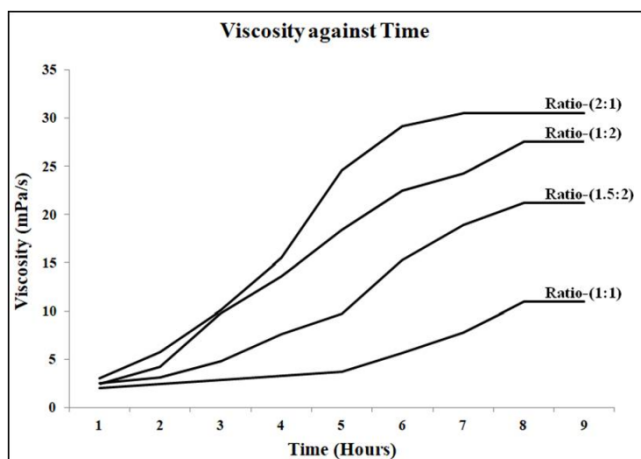


Fig. 4. Viscosity graph of different polysiloxane resins

The graph in Figure 4 shows a steady viscosity increment of Ratio-2:1. It gradually increased before steeply rose to 24.6 mPa/s. As time proceeds, the formations of amide linkages due to polymerization give different viscosity values for each sample. The process forms a reactive silanol

(Si-O-H) that reacts with a hydroxyl group (C-O-H), thus producing siloxane (Si-O-Si) bonds and amide linkages. The ethylene chain is next to the amide structure, and secondary amine nitrogen is integrated into an imidazoline ring [15]. Viscosity continues to rise until the reaction to produce amide linkage between the two oligomers is completely consumed, resulting in a constant viscosity value.

The viscosity for ratios 1:2 and 1.5:2 shows less increment before reaching the constant state at the 8th hour with a recorded value of 27.5 mPa/s and 21.2 mPa/s, respectively. Ratio 2:1 reached the constant state on the 7th hour with the highest viscosity value of 30.5 mPa/s which indicates the highest addition of amide linkage. Therefore, ratio 2:1 was selected as an ideal binder.

3.2. Determination of amine group amide linkages

The viscosity test result was supported by FTIR characterization as shown in Figure 5. The peaks for ratios 2:1, 1:2, and 1.5:2 shown at 3283 cm⁻¹, 3500 cm⁻¹, and 3345 cm⁻¹ respectively are attributed to hydroxyl groups (O-H) stretching vibrations with strong and sharp bonds belonging to the silane group.

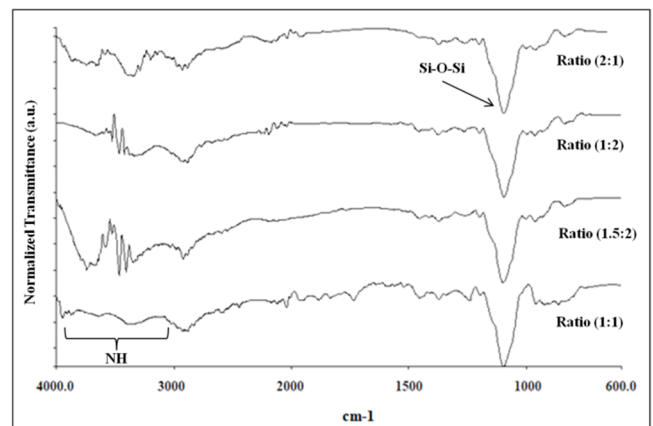


Fig. 5. FTIR spectrum of different polysiloxane resins

The peaks at 2923 cm⁻¹ (2:1), 2881 cm⁻¹ (1:2), and 2917 cm⁻¹ (1.5:2) correspond to the bands of alkane group (C-H) stretching vibrations with medium frequency bonds.

The sharp peak is shown at 1080 cm⁻¹ (2:1), 1091 cm⁻¹ (1:2), and 1100 cm⁻¹ (1.5:2), represents (Si-O-Si) stretching of siloxane functional group. These peaks are associated with the formation of amide linkage.

Similar assessments of silica materials reported that hydroxyl groups stretching modes are responsible at 3600 to 3000 cm⁻¹ and the band at 3425 cm⁻¹ is due to (-OH) hydrogen bond [16]. Silica has a distinctive area of peaks

ranging from 1250 to 700 cm^{-1} that offers a network of essential structural characteristics [16].

The tailored silanes showed strong peaks on a large scale with greater intensity compared to the control sample, indicating, a stronger crosslink network. All tailored samples showed an increment of siloxane bonds with higher concentrations.

3.3. Determination of particle size distribution and polydispersity index (PDI) of TiO_2

The size distribution and PDI of 10% (Nano-A), 20% (Nano-B), and 30% (Nano-C) (w/v) TiO_2 in dehydrated ethanol are presented in Table 1.

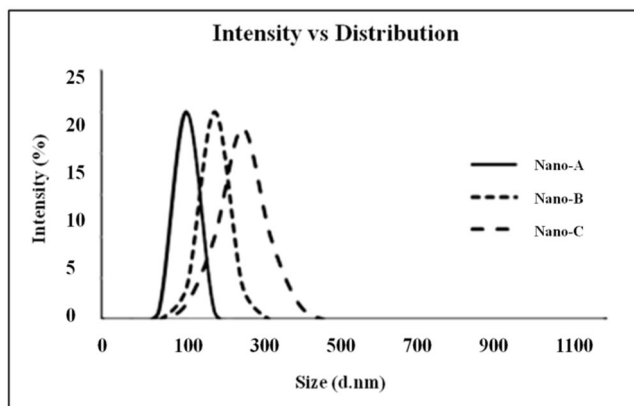


Fig. 6. Particle size measurement of TiO_2 dispersions

Clear coating is influenced by particle size. Smaller size decreases coating opacity, thus yielding more of its properties and efficiently scatters light. Size distributions by intensity are shown in Figure 6. All samples form Gaussian (normal) distribution with narrow width and single peak. Size distribution for Nano-A, B, and C shows that there are

Table 1. Percentile distribution of particle size and polydispersity index (PDI) data

Sample	10% Percentile distribution, nm	20% Percentile distribution, nm	30% Percentile distribution, nm	Polydispersity Index, PDI
Nano-A	87	99	156	1
Nano-B	99	224	283	6
Nano-C	167	289	367	10

Table 2. Curing test data

Sample	Resin-2:1	Resin-1:2	Resin-1.5:2
1 st Curing Phase: 'Dry-to-Touch', minutes	30	50	110
2 nd Curing Phase: 'Dry-to-Handle', minutes	180	360	490

10% of particles with distributions below 87 nm, 99 nm, and 167 nm, respectively. At median size distribution, the respected samples showed 50% of particles are below 99 nm, 224 nm, and 289 nm.

PDI defines the particle size range corresponding to the particle size distribution. Nano-A, B, and C recorded PDI values of 1, 6, and 10 respectively. The significant variation in PDI is due to the different intensities of polymerization. High PDI indicates less homogenous particle size. Based on the result, Nano-A was noted as the best dispersion.

3.4. Curing test

Different molar ratios of polysiloxane resins were firstly integrated with additives solution and were coated on glass substrates. Each was labelled as Resin-1:2, Resin-2:1 and Resin-1.5:2. Results were recorded in Table 2. Samples were cured through a condensation process.

The first curing period was defined as 'dry-to-touch'. The sample is considered dry if no prints are presented after being touched. The fastest drying time of 30 minutes was recorded by Resin-2:1. Resin-1:2 and Resin-1.5:2 took 50 minutes and more to dry, respectively. Second period was defined as 'dry-to-handle'. Sample is considered cured if distortion was not presented after being touched and handled. Resin-2:1 took 180 minutes (3 hours), 360 minutes (6 hours) for Resin-1:2, and 490 minutes (8 hours 10 minutes) for Resin-1.5:2 to completely harden, thus forming a polysiloxane network.

Condensation is part of the polymerization process that takes place via the silanol group (Si-OH) to form siloxane bridges (Si-O-Si) by removing water (H_2O) or alcohol from the polyamide network. The rate of condensation differs from one another as the process depends on numerous parameters such as the environment setting, chemical conditions, and the type of silane used [17].

When the resin is coated on glass, it causes an epoxy ring opening. The surface modification will occur on the inorganic surface of the glass to give better anchoring of the coating film. BF_3 catalyst promoter aids coating to cure at a much substantial rate.

Based on the curing analysis, Resin-2:1, containing the inorganic polysiloxane of Ratio-2:1, was chosen as an ideal polysiloxane resin to act as a coating binder.

3.5. Complete coating formulations (CF) performance in the hardness test

Complete coating formulations (CF) consist of an ideal coating binder (previously merged with the additives solutions of HBP and BF_3) along with different TiO_2 concentrations labelled as CF-A, CF-B and CF-C. Each sample was coated on glass substrates. For this comparative test, pencil grades from the same manufacturer were used. Following ASTM D3363, testing begins with the hardest pencil (6H) to the softest until the coating film is not scratched.

A recent study shows that surface coated with inorganic coatings gives little to moderate damage compared to uncoated surfaces, which bear the maximum damage [18]. Protective compositions of quartz (a silica-based mineral) and ceramic coat give low damage values for 4H and 6H hardness [18]. In this study, the quoted pencil hardness for CF-B (20% TiO_2) and CF-C (30% TiO_2) are 5H and 4H, respectively, with each being the hardest pencil grade that does not mark the surface of coated glass.

CF-A (10% TiO_2) shows excellent results, and 6H is quoted as the hardest pencil that did not scratch the coating film. The results coincide with the curing results, where a well-cured coating sample portrayed a harder film on the glass substrate. The smaller-sized TiO_2 also aids in improving the surface qualities thus, they exhibit better protection. Figure 7 shows the recorded data.

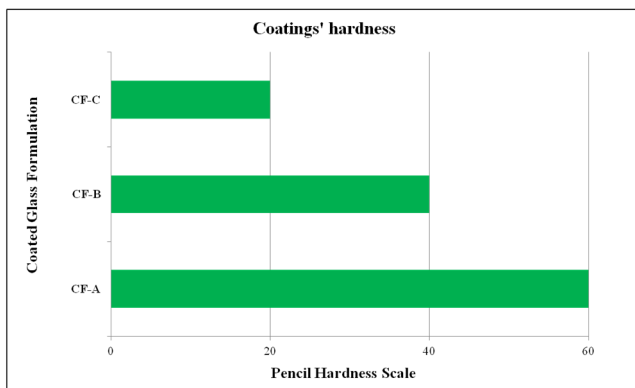


Fig. 7. Coatings' hardness data for each resin formulation

3.6. Complete coating formulations (CF) performance on the infrared transmission (IR%), ultraviolet transmission (UV%), and visible light transmission (VT%)

Samples for CF-A, CF-B, and CF-C (containing 10%, 20%, and 30% TiO_2 dispersions, respectively) were further tested for their filtration on solar energy transmission using WEP instrumentation shown in Figure 8 below. Obtained data are presented in Table 3.



Fig. 8. WEP instrument to analyse the UV, visible light, and IR transmission on coated glass

Table 3. Heat energy transmissions of complete coating formulations

Sample	UV% (100-400 nm)	VT% (400-700 nm)	IR% (> 700 nm)
CF-A	00	61	07
CF-B	15	73	15
CF-C	00	67	11

UV transmission measures the number of UV rays allowed to pass through cured coating film. The previous study analysed the performance of coated sample via UV-Vis, and TiO_2 -coated glass exhibited a reduction in transmittance. Glass coated with the highest TiO_2 concentration blocked 74.2% of UV light, and the lowest concentration blocked 57.3% of UV light [19]. This study showed that coated glass with the lowest TiO_2 concentration (CF-A) bears the same performance as the highest TiO_2 concentration (CF-C).

Both formulations blocked 100% UV transmission, while coated glass with the median TiO₂ concentration permits 15% UV transmission or 85% UV transmittance.

Literature with the use of WEP instruments to study TiO₂ coated glass on its performance towards UV, IR, and visible light transmission is not present. Therefore, literature [17] was used to convey the idea of TiO₂ performance in coating formulations.

Visible light transmittance (VT) measures the amount of daylight allowed to pass through the coated sample. High VT indicates low-tint samples and more visible light can pass through.

The previous study showed in the visible region of UV-VIS, glass coated with the highest TiO₂ concentration had a transmittance of 66.7%, and the lowest concentration of TiO₂ had a transmittance of 83.9% [19]. Results obtained in this study via WEP showed that all samples maximized at least 61% daylight (CF-A) and at most of 73% daylight (SC-B). Each sample exhibits a low tint coating of above 60% VT value. TiO₂ size reduction gives better coating transparency to maximize daylight while efficiently scatters visible light.

IR rays have a longer wavelength (400-700 nm). Radiated IR heat can be sensed physically. IR that passes through sample CF-A, CF-B, and CF-C were recorded at 7%, 15%, and 11% respectively. This explains that sample CF-A exhibits superior inner thermal comfort while the interior atmosphere of CF-B experienced the highest radiated heat, and CF-C gives off medium indoor comfort.

4. Conclusions

Transparent TiO₂ glass-based coating was successfully developed and tested for its performance. It was established that:

- 1) Sample Ratio-2:1 showed high viscosity value. High viscosity indicates high addition of amide linkages.
- 2) FTIR supported viscosity result. Strong peaks of amide linkages were presented by sample Ratio-2:1.
- 3) Particle size distribution of TiO₂ dispersion showed Nano-A exhibits the finest result of 87 nm for 10% percentile distribution with correlating PDI measurement of 1, indicating strongly homogenous particle size. Nano-A was noted as the best TiO₂ dispersion.
- 4) Resin-2:1 containing the additives solution and prepared inorganic polysiloxane resin of Ratio-2:1 exhibit the fastest curing time. Resin 2:1 was chosen as an ideal coating binder.
- 5) Pencil hardness test confirms that CF-A possesses hard coating property as the film does not scratch against 6H pencil grade.
- 6) WEP analysis conveyed that sample CF-A bearing Nano-A displayed superior performance by filtering 100% and 93% of UV and IR transmissions, respectively while maximizing daylight of 61%.
- 7) The addition of a catalyst inhibitor during the preparation of polysiloxane resin should be considered. Improvement in TiO₂ dispersion can be made to reach greater size reduction to exhibit more of its potential.
- 8) The obtained results from several analyses in this study, together with the findings from previous literature, conveyed that undemanding ways are also capable of developing good transparent TiO₂ glass-based coating.

Acknowledgements

The author would like to thank the Institute of Research Management and Innovation (IRMI), UiTM in providing the research funding grant of Bestari Perdana (Number: 600-IRMI/DANA5/3/BESTARI) and to Institute of Science (IOS), UiTM for their assistance in this research.

Additional information

The article was presented at the 5th ICET 2021: 5th International Conference on Engineering Technology Virtual Conference KEMAMAN, Malaysia, October 25-26, 2021.

References

- [1] R. Karanen, The Effect of Windows on Thermal Comfort, Degree Thesis, Arcada, 2016. Available from: <https://core.ac.uk/download/pdf/45600814.pdf>
- [2] E. Yousif, R. Haddad, Photodegradation and Photostabilization of Polymers, Especially Polystyrene: Review, SpringerPlus 2 (2013) 398. DOI: <https://doi.org/10.1186/2193-1801-2-398>
- [3] M. Brenner, V.J. Hearing, The Protective Role of Melanin Against UV Damage in Human Skin, Photochemistry and Photobiology 84/3 (2008) 539-549. DOI: <https://doi.org/10.1111/j.1751-1097.2007.00226.x>
- [4] T. Herrling, K. Jung, J. Fuchs, UV - Generated Free Radicals (FR) in Skin and Hair - Their Formation, Action, Elimination and Prevention. A general review, SOFW-Journal 133/8 (2007) 2-11.
- [5] J. Rommens, A. Verhaege, G. Michiels, M. Diebold, TiO₂ Impact on Paint Weather Resistance, Coatings World. Access in: 15.09.2021, Available from:

- https://www.coatingsworld.com/issues/2017-09-01/view_features/tio2-impact-on-paint-weather-resistance/
- [6] R.V.D. Belt, E. Currie, Dispersion of Nanoparticles in Organic Solvents, United States Patent Application Publication, 9 December 2010. Access in: 10.12.2020, Available from: <https://patentimages.storage.googleapis.com/3d/0d/06/834fdb17230481/US8333831.pdf>
- [7] N. Liu, J. Yu, Y. Meng, Y. Liu, Hyperbranched polysiloxanes based on polyhedral oligomeric silsesquioxane cages with ultra-high molecular weight and structural tuneability, *Polymers* 10/5 (2018) 496. DOI: <https://doi.org/10.3390/polym10050496>
- [8] R.P.D. Melo, V.D.O. Aguiar, M.D.F.V. Marques, Silane Crosslinked Polyethylene from Different Commercial PE's: Influence of Comonomer, Catalyst Type and Evaluation of HLPB as Crosslinking Coagent, *Materials Research* 18/2 (2015) 313-319. DOI: <https://doi.org/10.1590/1516-1439.303214>
- [9] K. Hughes, Professional Painting Knowledge Base Inorganic Coatings for Industrial Projects. Performance Painting: Prepare, Protect, Preserve, 30 October 2018. Access in: 9.12.2020, Available from: <https://www.performance-painting.com>
- [10] J. Liu, Q. Xu, F. Shi, S. Liu, J. Luo, L. Bao, Dispersion of $\text{Cs}_{0.33}\text{WO}_3$ Particles for Preparing its Coatings with Higher Near Infrared Shielding Properties, *Applied Surface Science* 309 (2014) 175-180. DOI: <https://doi.org/10.1016/j.apsusc.2014.05.005>
- [11] X. Chen, S. Zhou, B. You, Ambient-curable Polysiloxane Coatings: Structure and Mechanical Properties, *Journal of Sol-Gel Science and Technology* 58 (2011) 490-500. DOI: <https://doi.org/10.1007/s10971-011-2418-7>
- [12] Y. Liu, Z. Yu, S. Zhou, L. Wu, De-agglomeration and Dispersion of Nano-TiO₂ in an Agitator Bead Mill, *Journal of Dispersion Science and Technology* 27/7 (2006) 983-990. DOI: <https://doi.org/10.1080/01932690600766975>
- [13] G. Georgiev, T. Dikova, Hardness Investigation of Conventional Bulk Fill and Flowable Dental Composites, *Journal of Achievements in Material and Manufacturing Engineering* 109/2 (2021) 68-77. DOI: <https://doi.org/10.5604/01.3001.0015.6261>
- [14] P.T. Iswanto, H. Akhyar, A. Faqihudin, Effect of Shot Peening on Microstructure, Hardness, and Corrosion Resistance of AISI 316L, *Journal of Achievements and Material Manufacturing Engineering* 89/1 (2018) 19-26. DOI: <https://doi.org/10.5604/01.3001.0012.6668>
- [15] J. Koleske (ed), *Paint and Coating Testing Manual*, 15th Edition, ASTM International, Pennsylvania, 2012.
- [16] L.B. Capeletti, J.H. Zimnoch, Fourier Transform Infrared and Raman Characterization of Silica-Based Materials, in: M.T. Stauffer (ed), *Applications of Molecular Spectroscopy to Current Research in the Chemical and Biological Sciences*, IntechOpen, London, 2016, 5-22. DOI: <http://dx.doi.org/10.5772/64477>
- [17] A.A. Issa, A.S. Luyt, Kinetics of Alkoxysilanes and Organoalkoxysilanes Polymerization: A Review, *Polymers* 11/3 (2019) 537. DOI: <https://doi.org/10.3390/polym11030537>
- [18] A. Avakov, E. Kosenko, I. Topilin, F. Kopilov, Analysis of methods of assessing the quality of protective paint car coatings, *MATEC Web of Conferences* 224 (2018) 02103. DOI: <https://doi.org/10.1051/mateconf/201822402103>
- [19] W. Johansson, A. Peralta, B. Jonson, S. Anand, L. Österlund, S. Karlsson, Transparent TiO₂ and ZnO Thin Films on Glass for UV Protection of PV Modules, *Frontier in Materials* 6 (2019) 259. DOI: <https://doi.org/10.3389/fmats.2019.00259>



© 2022 by the authors. Licensee International OCSCO World Press, Gliwice, Poland. This paper is an open access paper distributed under the terms and conditions of the Creative Commons Attribution-NonCommercial-NoDerivatives 4.0 International (CC BY-NC-ND 4.0) license (<https://creativecommons.org/licenses/by-nc-nd/4.0/deed.en>).